Dual mTORC1/2 inhibition sensitizes testicular cancer models to cisplatin treatment

Rosas-Plaza, Ximena; de Vries, Gerda; Meersma, Gert Jan; Suurmeijer, Albert J H; Gietema, Jourik A; van Vugt, Marcel A T M; de Jong, Steven

Published in:
Molecular cancer therapeutics

DOI:
10.1158/1535-7163.MCT-19-0449

Publication date:
2020

Published OnlineFirst November 19, 2019; DOI: 10.1158/1535-7163.MCT-19-0449

Dual mTORC1/2 Inhibition Sensitizes Testicular Cancer Models to Cisplatin Treatment

Ximena Rosas-Plaza[1], Gerda de Vries[1], Gert Jan Meersma[1], Albert J.H. Suurmeijer[2], Jourik A. Gietema[1], Marcel A.T.M. van Vugt[1], and Steven de Jong[1]

ABSTRACT

Testicular cancer is the most common cancer type among young men. Despite highly effective cisplatin-based chemotherapy, around 20% of patients with metastatic disease will still die from the disease. The aim of this study was to explore the use of kinase inhibitors to sensitize testicular cancer cells to cisplatin treatment. Activation of kinases, including receptor tyrosine kinases and downstream substrates, was studied in five cisplatin-sensitive or -resistant testicular cancer cell lines using phospho-kinase arrays and Western blotting. The phospho-kinase array showed AKT and S6 to be among the top phosphorylated proteins in testicular cancer cells, which are part of the PI3K/AKT/mTORC pathway. Inhibitors of most active kinases in the PI3K/AKT/mTORC pathway were tested using apoptosis assays and survival assays. Two mTORC1/2 inhibitors, AZD8055 and MLN0128, strongly enhanced cisplatin-induced apoptosis in all tested testicular cancer cell lines. Inhibition of mTORC1/2 blocked phosphorylation of the mTORC downstream proteins S6 and 4E-BP1. Combined treatment with AZD8055 and cisplatin led to reduced clonogenic survival of testicular cancer cells. Two testicular cancer patient-derived xenografts (PDX), either from a chemosensitive or -resistant patient, were treated with cisplatin in the absence or presence of kinase inhibitor. Combined AZD8055 and cisplatin treatment resulted in effective mTORC1/2 inhibition, increased caspase-3 activity, and enhanced tumor growth inhibition. In conclusion, we identified mTORC1/2 inhibition as an effective strategy to sensitize testicular cancer cell lines and PDX models to cisplatin treatment. Our results warrant further investigation of this combination therapy in the treatment of patients with testicular cancer with high-risk relapsed or refractory disease.

Introduction

Testicular cancer is the most frequent cancer type among young men (20–40 years). Incidence of testicular cancer in the Western world has risen steadily over the past 40 years and even tripled in Northern European countries (1). Localized disease is treated with surgery with a >97% cure rate (2). Survival of patients with testicular cancer with advanced disease is much higher when compared with other tumor types, with an approximately 80% survival rate (3). However, there is a subset of patients that does not respond to cisplatin-based chemotherapy and will eventually die from this disease. Several features have been proposed to underlie the pronounced cisplatin sensitivity in testicular cancer, among others the high percentage of tumors with wild-type *TP53* status and the low expression levels of the nucleotide excision repair (NER) proteins ERCC1, XPF, and XPA (4). Cisplatin treatment of testicular cancer induces apoptosis by increasing the cellular levels of p53, a transcription factor that can activate both the intrinsic apoptotic pathway via PUMA and NOXA and the extrinsic apoptotic pathway by inducing the expression of death receptors on the cell membrane (5–7).

Mutation-driven activation of members from the PI3K/AKT/mTOR complex (mTORC) pathway, among other prosurvival pathways, is observed in many cancers (8, 9). However, almost no mutations in PI3K/AKT/mTORC pathway components or upstream receptor tyrosine kinases have been found in either cisplatin-sensitive or -resistant testicular cancers (10–12). Nonetheless, it was previously described that PI3K or AKT inhibition sensitized cisplatin-resistant testicular cancer cells to cisplatin (13). In addition, specific receptor tyrosine kinase (RTK) activity was investigated in testicular cancer cell lines, identifying IGF1R as therapeutic target (14). However, other upstream kinases causing activation of the PI3K/AKT pathway or involvement of other intracellular kinases in resistance mechanisms against cell death were not evaluated in depth.

In this study, we screened a panel of cisplatin-sensitive and -resistant testicular cancer cell lines to determine the phosphorylation status of kinases and their downstream targets using phospho-arrays. On the basis of these results, we screened a number of kinase inhibitors alone and in combination with cisplatin, using apoptosis induction as readout of sensitization. Inhibition of mTORC1/2 strongly enhanced cisplatin-induced apoptosis in sensitive and resistant testicular cancer cell lines as well as patient-derived xenografts (PDX).

Materials and Methods

Cell lines

Testicular cancer embryonal carcinoma cell lines Tera, TeraCP, Scha, 833KE, and NCCIT were cultured in RPMI (Gibco), supplemented with 10% FCS (Life Technologies). Cell lines were maintained at 37°C in a humidified incubator with 5% CO_2. All cell lines grew adherent and were passaged twice weekly. All cell lines were tested by short tandem repeat profiling at Eurofins Genomics and were *Mycoplasma* free.

[1]Department of Medical Oncology, Cancer Research Center Groningen, University of Groningen, University Medical Center Groningen, Groningen, the Netherlands. [2]Department of Pathology, Cancer Research Center Groningen, University of Groningen, University Medical Center Groningen, Groningen, the Netherlands.

Note: Supplementary data for this article are available at Molecular Cancer Therapeutics Online (http://mct.aacrjournals.org/).

X. Rosas-Plaza and G. de Vries contributed equally to this article.

Corresponding Author: Steven de Jong, Cancer Research Center Groningen, University Medical Center Groningen, University of Groningen, Hanzeplein 1, 9713GZ Groningen, the Netherlands. Phone: 315-0361-2964; Fax: 315-0361-4862; E-mail: s.de.jong@umcg.nl

Mol Cancer Ther 2020;19:590–601

doi: 10.1158/1535-7163.MCT-19-0449

Published OnlineFirst November 19, 2019; DOI: 10.1158/1535-7163.MCT-19-0449

RTK signaling antibody array

The PathScan RTK Signaling Antibody Arrays (#7949; Cell Signaling Technology), thereafter referred to as "phospho-arrays," were used according to the manufacturer's instructions. Scha, Tera, or TeraCP cells were lysed and protein concentration was determined using Bradford assay. Membranes were incubated with 75 µL (1 µg/µL) of protein extract. Image Studio Lite software (LI-COR) was used for data analysis.

Western blot analysis

Cell lysis was performed using mammalian protein extraction reagent (Thermo Fisher Scientific), supplemented with protease and phosphatase inhibitor cocktail (Thermo Fisher Scientific). Protein concentration was determined by a Bradford assay, after which 20 to 40 µg of protein extract was subjected to SDS-PAGE separation. Protein gels were then transferred to polyvinylidene fluoride membranes (Millipore) and blocked in 5% skimmed milk (Sigma) or 5% BSA (Serva) in TBS-0.05% Tween20 (Sigma). The following primary antibodies were used: AKT (#9272), p-AKT Ser473 (#9271), p-AKT Thr308 (#9275), S6 Ribosomal Protein (#2217), p-S6 Ribosomal Protein Ser235/236 (#2211), SRC (#2109), p-SRC Tyr419 (#2101), p-SRC Tyr530 (#2105), PDGFRß (#4564), 4E-BP1 (#9644), p-4E-BP1 Thr70 (#9455), LC3I/II (#4108), mTOR (#2972), Raptor (#22805), cleaved PARP (#5625), cleaved caspase-8 (#9496), cleaved caspase-9 (#9501), and cleaved caspase-3 (#9661) were all from Cell Signaling Technology. Actin (#69100) was from MP Biomedicals, HSP90 (sc-1055) was from Santa Cruz Biotechnology, and Rictor (#A300-459A) from Bethyl Laboratories. Membranes were incubated with horseradish peroxidase (HRP)-conjugated secondary antibodies (DAKO) and visualized using Lumi-light (Roche).

3-(4,5-Dimethylthiazol-2-yl)-2, 5 diphenyltetrazolium assay

Cells were plated in 96-well plates at a density of 5,000 cells/well for Tera, TeraCP, and 833KE, and 7,000 cells/well for Scha and NCCIT. At 2 to 3 hours after plating cells, one of the following agents was added, cisplatin (Accord Healthcare), Everolimus (Santa Cruz Biotechnology), GDC-0941, MK-2206, AZD8055, MLN0128 (also known as TAK-228; all from Axon Medchem), and dasatininb (Selleckchem). After a 96-hour incubation, 3-(4,5-dimethylthiazol-2-yl)-2, 5 diphenyltetrazolium (MTT; Sigma) was added at a concentration of 5 mg/mL for 4 hours. Medium was removed and the formazan crystals were dissolved in DMSO (Sigma). Absorbance was measured at 520 nm using an iMARK microplate absorbance reader (Bio-Rad). Relative survival was determined as the decrease in signal compared with untreated cells.

RNA interference of mTOR, Raptor, and Rictor

siRNA sequences: Raptor 5′- AAGGCTAGTCTGTTTCGAAAT-3′ (sense), 5′- AAGGCUAGUCUGUUUCGAAAU-3′ (antisense); Rictor 5′- AAACTTGTGAAGAATCGTATC-3′ (sense), 5′- AAACUUGUGAAGAAUCGUAUC-3′ (antisense). siRNAs were purchased from Eurogentec. Silencer predesigned siRNA against mTOR-I (145119), mTOR-II (242387), and Silencer Negative Control #1 were purchased from Invitrogen. Testicular cancer cells were transfected at approximately 50% confluency using 10 µL of siRNA duplexes (20 µmol/L), OPTI-MEM, and oligofectamine reagent according to manufacturer's instructions (Invitrogen).

Clonogenic survival assay

Wells were precoated with a mixture of 0.5% agar (Merck) in DMEM: F12 (Gibco) supplemented with 20% FCS. Cells were plated in 6-well plates at a density of 3,000 cells/well for Scha and 7,000 cells/well for TeraCP, in 0.3% agarose (Lonza), DMEM: F12 with 20% FCS. AZD8055 was added to the agarose cell mixture, whereas cisplatin treatment was performed for 24 hours prior to plating, and washed out before plating. Colonies were counted after 10 to 12 days. Clonogenic survival was determined as the relative decrease in colony formation compared with untreated cells. Colonies were stained with MTT (5 mg/mL) for 4 hours.

Flow cytometry

To measure apoptosis, cells were plated and left to adhere overnight after which drugs were added for 24 hours. Hexamethylindodicarbocyanine iodide (DilC) 1(5)/propidium iodide (PI) staining was performed according to manufacturer's instructions with final concentrations of 6 nmol/L and 0.2 µg/mL, respectively (Invitrogen). A total of 10,000 events per sample were analyzed on a FACSCalibur (BD Biosciences). FlowJo software was used for data analysis. The following autophagy inhibitors were used: SBI-0206965 (MedChem Express), Bafilomycin A1 (Sigma), and Chloroquine (InvivoGen).

Alternatively, intracellular staining of cleaved caspase-3 was performed to quantify apoptosis. Cells were plated and left to adhere overnight. Cells were treated for 24 hours, in the presence or absence of Benzyloxycarbonyl-Val-Ala-Asp (OMe) fluoromethylketone (Z-VAD-FMK, 20 µmol/L; Promega). Cells were then fixed in 4% paraformaldehyde, permeabilized using 100% ice cold methanol (MeOH; Sigma), and stained for cleaved caspase-3 (#9661; Cell Signaling Technology) in FACS buffer (1× PBS, 0.1% Tween-20, 1% BSA). Secondary antibody labeling was performed using Alexa Fluor 488–conjugated goat anti-rabbit (Invitrogen) in FACS buffer. Cells were analyzed on a BD Accuri C6 flow cytometer (BD Biosciences). FlowJo software was used for data analysis.

IHC

IHC was performed on formalin-fixed paraffin-embedded tissue. Tissue slides were deparaffinized in xylene and rehydrated in ethanol. Antigen retrieval was done using citrate buffer (pH 6.0) or EDTA buffer (pH 8.0) for 15 minutes. Endogenous peroxidase was blocked for 30 minutes with 0.3% H_2O_2. Tissue slides were then incubated with the primary antibodies diluted in PBS, 1% BSA for 1 hour at room temperature or overnight at 4°C. Slides were stained with HRP-labeled secondary antibodies (DAKO). Staining was visualized by 3,3′-diaminobenzidine and counterstained with hematoxylin. Primary detection antibodies that were used: p-S6 Ribosomal Protein Ser235/236 (#2211; Cell Signaling Technology), p-4E-BP1 Thr37/46 (#2855), Ki-67 (#M7240; DAKO), and cleaved caspase-3 (#9661; Cell Signaling Technology). Analysis of IHC stainings was performed on whole tissue sections using Aperio ImageScope (Leica Biosystems).

In vivo studies

All animal experiments were approved by the Institutional Animal Care and Use Committee of the University of Groningen (Groningen, the Netherlands). Written informed consent was obtained before surgery from all patients of which tumor samples were used for PDX establishment. Tumor tissues were implanted and propagated successfully according to previously described methods (15). In short, tumor pieces were cut into 3 × 3 × 3 mm sections and subcutaneously implanted in the flank of 4- to 8-week-old NOD.Cg-Prkdcscid Il2rgtm1Wjl/SzJ (NSG) male mice (internal breed; Central Animal Facility, University Medical Centre Groningen, the Netherlands). Two nonseminoma PDX models (*TP53* wild-type, as determined with sequencing) were used, TC1 and TC4. TC1 was established from a

Published OnlineFirst November 19, 2019; DOI: 10.1158/1535-7163.MCT-19-0449

primary tumor with embryonal carcinoma, yolk sac tumor, and teratoma components. TC4 was established from biopsy material obtained from a retroperitoneal lesion. Pathologic evaluation showed that TC1 consisted of yolk sac tumor and immature teratoma components, and TC4 belonged to the yolk sac histologic subtype. Tumor growth was quantified three times a week by caliper measurements according to the formula (width^2 × length)/2. When tumors demonstrated sustained growth, mice were randomized into vehicle control or treatment groups (n = 4–6 mice/group). AZD8055 (10 mg/kg in 10% DMSO), 40% polyethylene glycol 300 (Sigma), or vehicle were administered daily. Cisplatin (2.5–4 mg/kg) was administered weekly. All treatments were done via intraperitoneal injection. All mice were sacrificed after 21 days of treatment, or when a tumor volume of 1,500 mm^3 (humane endpoint) was reached. Tumor growth was depicted as the change in tumor volume (mm^3) by subtracting initial tumor volume from tumor volume at the end of treatment. For *ex vivo* analysis the tumors were resected, formalin fixed, and paraffin embedded.

Statistical analysis

In vitro data are expressed as mean ± SD or SEM of at least three individual experiments. GraphPad Prism was used for data analysis. *T* tests and one- or two-way ANOVA were used to compare means between all groups and the *post hoc* Dunnett or Sidak test was performed to determine statistical differences between two groups.

Results

The PI3K/AKT/mTORC pathway is highly active in testicular cancer cell lines

An intrinsic cisplatin-resistant testicular cancer model (Scha) and an acquired cisplatin-resistant testicular cancer model (TeraCP), and its sensitive parental model (Tera) were used to identify the activation status of kinases and their downstream targets (Supplementary Fig. S1A). A RTK phospho-array was performed to determine the phosphorylation levels of 29 RTKs and 10 downstream substrates involved in the PI3K/AKT/mTORC, MAPK, and JAK/STAT pathways (**Fig. 1A**). The phosphorylation status of SRC (panTyr), S6 (Ser235/236), AKT (Thr308), and AKT (Ser473; **Fig. 1C**) and the RTKs FGFR1 (panTyr), HER2 (panTyr), and HER3 (panTyr; **Fig. 1B**) showed the highest mean relative fluorescence intensity for the three testicular cancer models. Phosphorylation levels of p-S6, p-AKT^{308}, and p-AKT^{473} were validated (Supplementary Fig. S1B). Scha, Tera, and TeraCP showed similar levels of S6 and AKT phosphorylation both in the RTK phospho-array and with Western blotting. To examine whether the activating or the inactivating phosphorylation site of SRC was phosphorylated, levels of p-Tyr^{419} (activating) and p-Tyr^{530} (inactivating) were determined. Both sites were highly phosphorylated in intrinsic resistant Scha cells, and to a lesser extent in Tera and TeraCP cells. We included two additional testicular cancer cell lines, the cisplatin-sensitive 833KE cell line and cisplatin-resistant *TP53*-mutant NCCIT cell line (Supplementary Fig. S1A). 833KE cells showed low p-AKT and p-SRC levels, when compared with those of Scha, Tera, and TeraCP cells. NCCIT cells showed high phosphorylation levels of all aforementioned phospho-sites (Supplementary Fig. S1B). S6 phosphorylation levels in 833KE and NCCIT cells were similar to those in Scha, Tera, and TeraCP cells.

Testicular cancer cells lines are highly sensitive to mTORC1/2 inhibition

Sensitivity of testicular cancer cells toward inhibitors targeting kinases previously identified as being active in Scha, Tera, and TeraCP was evaluated with MTT assays. Despite the high phosphorylation levels of SRC, testicular cancer cells were not sensitive to SRC inhibition using dasatinib (**Fig. 1D**). Testicular cancer cells showed higher sensitivity to PI3K inhibitor GDC-0941 and AKT inhibitor MK-2206 (**Fig. 1E** and **F**). Importantly, all testicular cancer cell lines exhibited similarly high sensitivity to mTORC1/2 inhibitors AZD8055 and MLN0128 (**Fig. 1H** and **I**). Both mTORC1/2 inhibitors greatly affected survival of testicular cancer cells in comparison with the mTORC1 inhibitor everolimus (**Fig. 1G**).

mTORC1/2 inhibition effectively sensitizes testicular cancer cell lines to cisplatin

Cisplatin is a strong inducer of apoptosis both *in vitro* and *in vivo* in testicular cancer models (16). Therefore, we tested whether inhibition of PI3K/AKT/mTORC pathway kinases or SRC could enhance cisplatin-induced cell death. To this end, we screened a panel of drugs (GDC-0941, MK-2206, everolimus, AZD8055, and MLN0128) in TeraCP and Scha cells when used in combination with cisplatin. Apoptosis and cell death was analyzed using flow cytometric analysis of DilC1(5)/PI staining. Inhibitor concentrations used in combination with cisplatin were chosen based on the concentration at which each cell line suffered minimal apoptosis inducing effects (**Fig. 2A**, **D**, and **G**). Scha cells were sensitized to cisplatin only upon addition of mTORC1/2 inhibitors (**Fig. 2A**). TeraCP cells were sensitized to cisplatin by all inhibitors (**Fig. 2D**). Notably, dasatinib sensitized TeraCP to cisplatin treatment, but did not alter cisplatin sensitivity of Scha cells (Supplementary Figs. S2A and S2B), even though SRC phosphorylation was already completely abolished at low concentrations (Supplementary Figs. S2C and S2D). Therefore, SRC inhibition was not further studied.

Induction of caspase-3 and PARP cleavage, two additional markers of apoptosis, was determined after treatment with the mTORC1/2 inhibitor AZD8055, cisplatin, or the combination. Cleavage of caspase-3 and PARP were observed after cisplatin treatment in TeraCP, and were elevated in both cell lines after the combination treatment (**Fig. 2H**). In addition to pharmacologic inhibition of mTOR, the effect of siRNA-mediated knockdown of mTOR, Raptor, or Rictor, specific components of mTOR complex 1 and complex 2 respectively, were investigated. Robust depletion of mTOR, Rictor, or Raptor knockdown was achieved, but almost no decrease in phosphorylated S6 or 4E-BP1, two downstream effectors of mTORC1, was found (Supplementary Fig. S3A). In addition, no major effects on apoptosis were observed in response to cisplatin treatment when mTOR, Rictor, or Raptor were downregulated (Supplementary Fig. S3B). These results suggest that strong downregulation of p-S6 and p-4E-BP1, as can be achieved with chemical inhibitors, is essential for enhancing apoptosis by cisplatin treatment.

Next, we investigated the PI3K/AKT/mTORC pathway activity in Scha and TeraCP at the molecular level. We specifically found a strong downregulation of p-AKT^{308}, p-AKT^{473}, and a modest downregulation of p-S6 and p-4E-BP1 (Thr70) in response to treatment with the PI3K inhibitor GDC-0941 and the AKT inhibitor MK-2206 (**Fig. 2B** and **E**). In line with expectation, inhibition of mTORC1 using everolimus resulted in a reduction in phosphorylation of S6 and 4E-BP1 (**Fig. 2B** and **E**). Interestingly, treatment with everolimus prompted an upregulation of p-AKT^{308} and p-AKT^{473} levels. This upregulation is strongly diminished in cells that were treated with AZD8055 or MLN0128, as demonstrated by reduced levels of p-AKT^{473} and, to a lesser extent, p-AKT^{308} (**Fig. 2B** and **E**). These results indicate that AZD8055 and MLN0128 more effectively inhibit the PI3K/AKT/mTORC pathway when compared with everolimus. This notion was

Published OnlineFirst November 19, 2019; DOI: 10.1158/1535-7163.MCT-19-0449

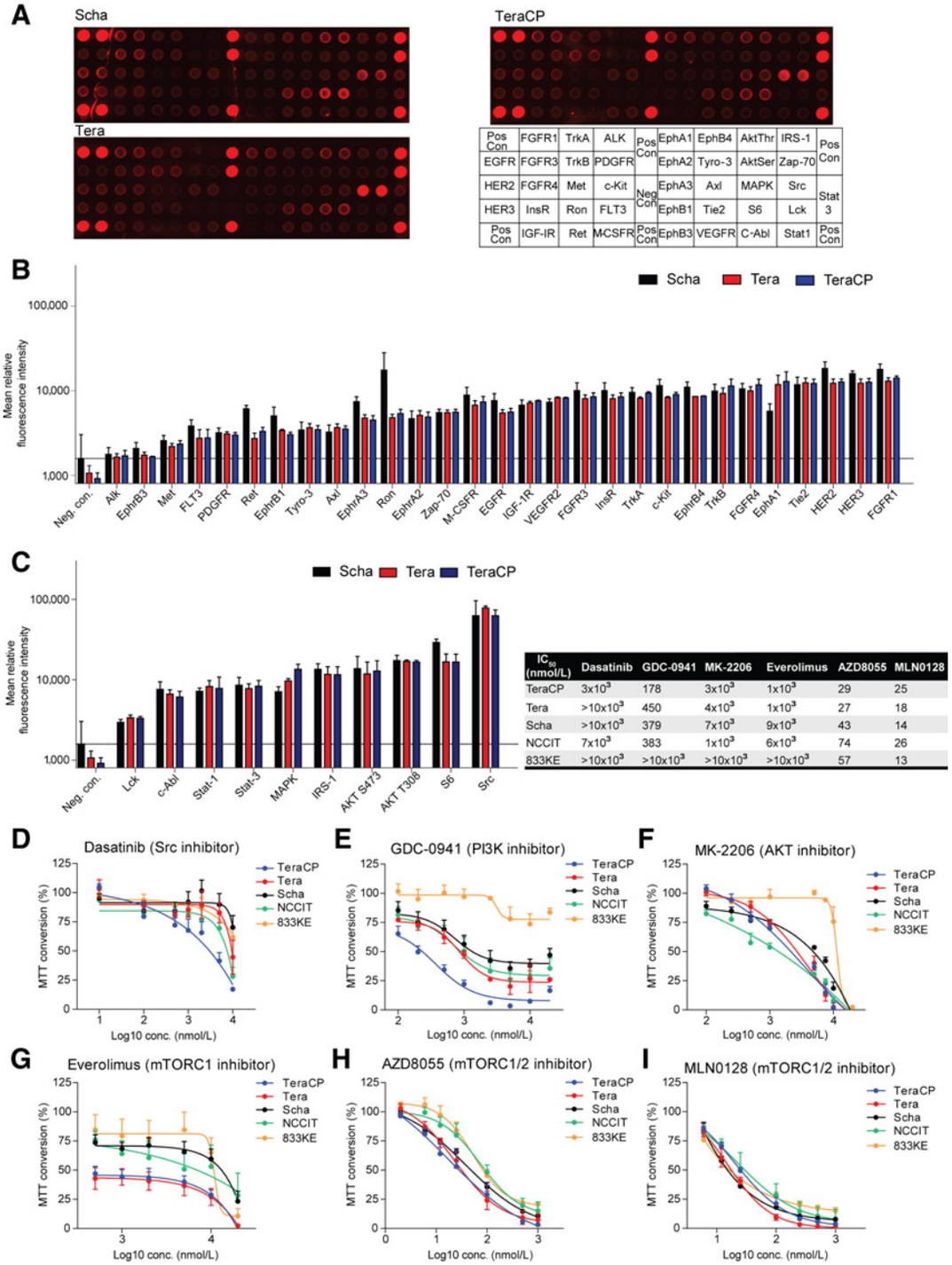

Figure 1.

Receptor tyrosine kinase screen and pharmacologic inhibition of kinases in testicular cancer cells. **A,** Representative image of phosphoarrays performed with Scha, Tera, and TeraCP cells and the schematic arrangement of the array. **B** and **C,** Mean fluorescence intensity of phosphorylated kinases and receptor tyrosine kinases. **D–I,** MTT survival assays and IC_{50} determined for testicular cancer cell lines: Tera, TeraCP, Scha, NCCIT, and 833KE treated with dasatinib, GDC-0941, MK-2206, everolimus, AZD8055, and MLN0128 for 96 hours. Data show average and ±SEM of three biological replicates.

Published OnlineFirst November 19, 2019; DOI: 10.1158/1535-7163.MCT-19-0449

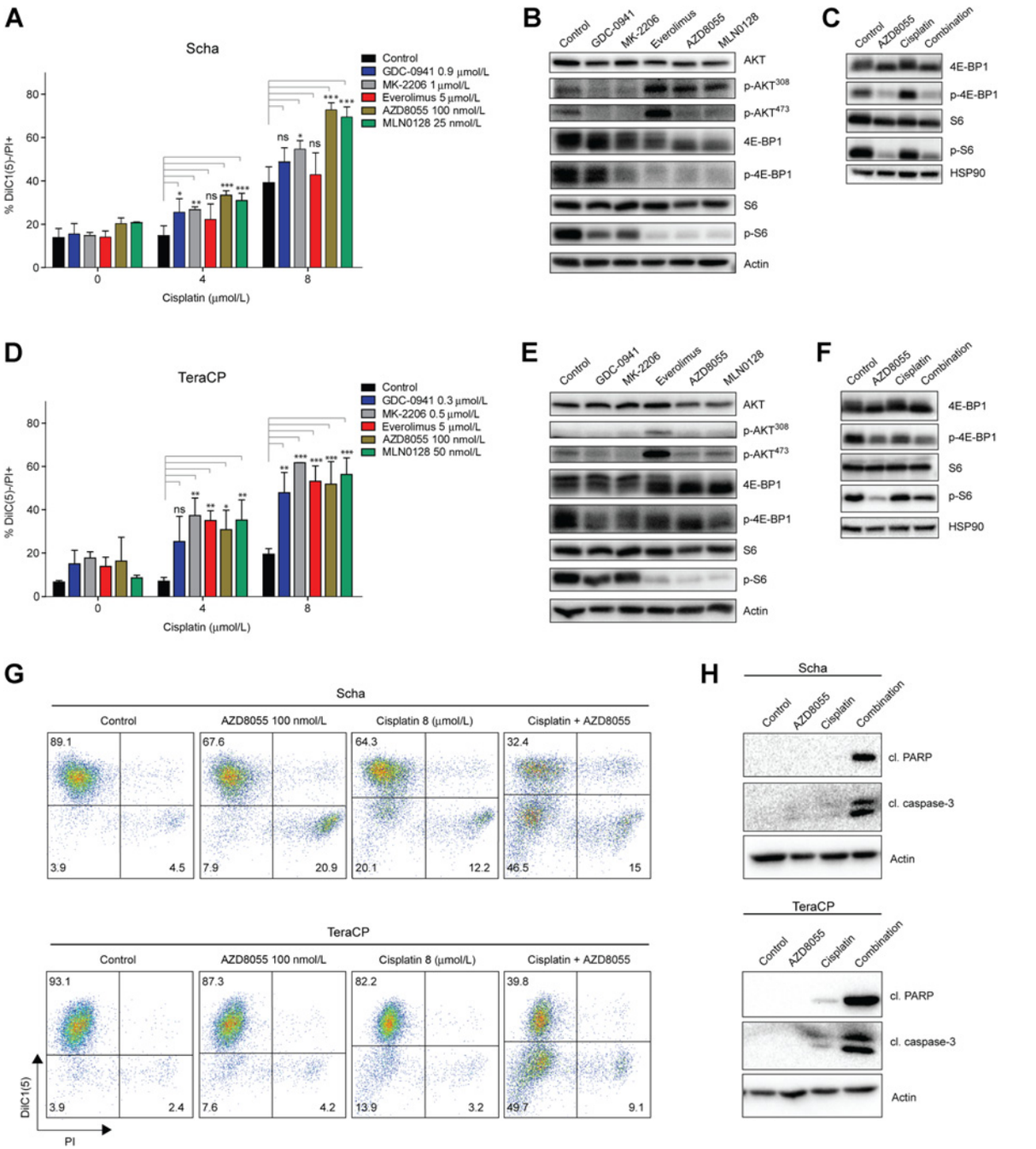

Figure 2.

mTORC1/2 inhibition in combination with cisplatin in resistant testicular cancer cells. **A** and **D**, Mean percentage of DILC1(5)−/PI−/+ Scha and TeraCP cells treated with 4 or 8 μmol/L of cisplatin alone or in combination with GDC-0941, MK-2206, everolimus, AZD8055, or MLN0128. On the *x*-axis, untreated and cisplatin-treated cells alone or in combination with the inhibitors; on the *y*-axis, the percentage of DiLC1(5)−/PI+ cells. Data show average and ±SD of three different replicates. ANOVA was used to test significance, and pairwise comparisons were done using Dunnett *post hoc* test. **B** and **E,** Representative Western blot image of Scha and TeraCP showing levels of AKT, p-AKT^{308}, p-AKT^{473}, S6, p-S6, 4E-BP1, and p-4E-BP1 after 24 hours of treatment with the inhibitors. **C** and **F,** Representative Western blot analysis of Scha and TeraCP cells showing levels of 4E-BP1, p-4E-BP1, S6, p-S6, and HSP90 after 24 hours of treatment with 100 nmol/L of AZD8055 and/or 4 μmol/L of cisplatin. **G,** DILC1(5)/PI staining of Scha and TeraCP cells treated for 24 hours with cisplatin alone or in combination with 100 nmol/L of AZD8055 and/or 8 μmol/L cisplatin. **H,** Representative Western blots of Scha and TeraCP showing levels of cleaved caspase-3 and cleaved PARP after 24 hours of treatment with AZD8055 (100 nmol/L), cisplatin (4 μmol/L), or the combination thereof. *, $P < 0.05$; **, $P < 0.01$; ***, $P < 0.001$; ns, not significant.

Published OnlineFirst November 19, 2019; DOI: 10.1158/1535-7163.MCT-19-0449

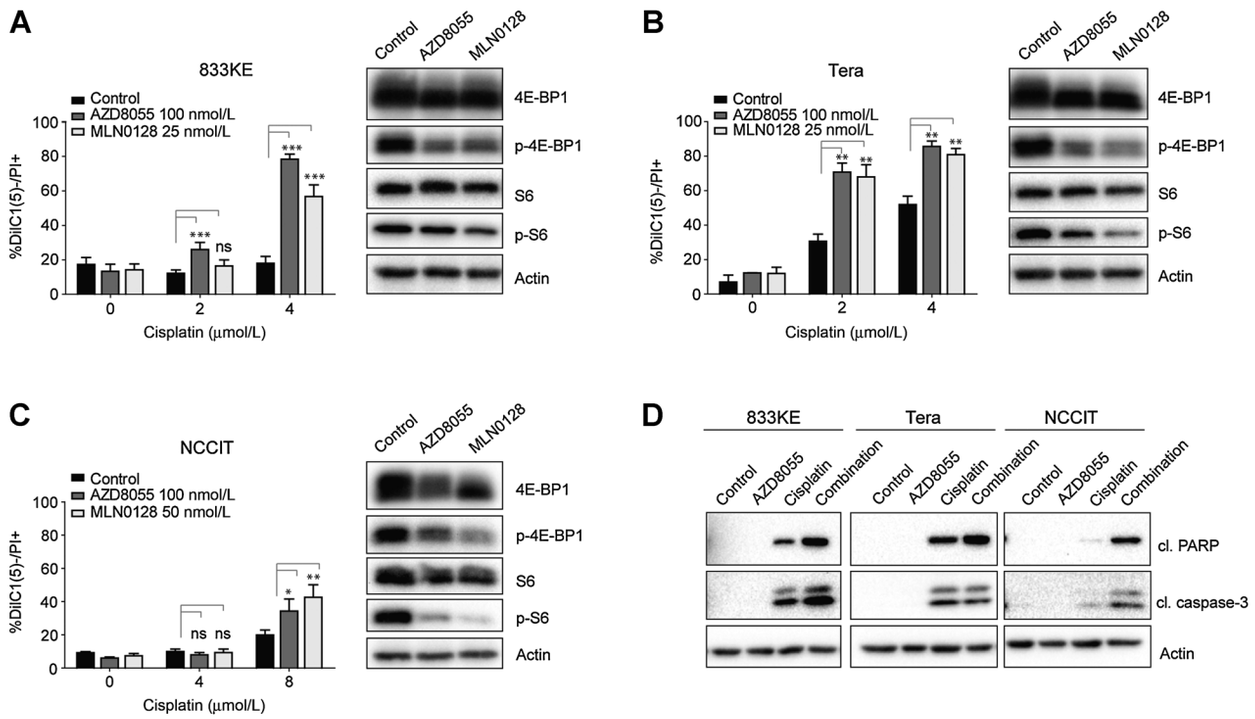

Figure 3.

Testicular cancer sensitization to cisplatin using mTORC1/2 inhibition in an additional panel of testicular cancer cell lines. **A–C,** Mean percentage of apoptotic and death cells and Western blot using 833KE, Tera, and NCCIT treated with AZD8055 and MLN0128 and/or cisplatin. Data show average and ± SD of three different replicates. ANOVA was used to test significance, and pairwise comparisons were done using Dunnett *post hoc* test. Representative Western blot image showing levels of S6, p-S6, 4E-BP1, p-4E-BP1, and actin after 24 hours of treatment with the AZD8055 or MLN0128. **D,** Representative Western blots of Tera, 833KE, and NCCIT showing levels of cleaved caspase-3 and cleaved PARP after 24 hours of treatment with AZD8055 (100 nmol/L), cisplatin (Tera and 833KE: 2 μmol/L; NCCIT: 8 μmol/L), or the combination thereof. *, $P < 0.05$; **, $P < 0.01$; ***, $P < 0.001$; ns, not significant.

further underscored by the strong loss of p-S6 and p-4E-BP1 in Scha and TeraCP cells treated with the combination of cisplatin and AZD8055 (**Fig. 2C** and **F**).

mTORC1/2 inhibitors sensitize both cisplatin-sensitive and -resistant testicular cancer cells to cisplatin

We tested the combination of cisplatin and AZD8055 in the other testicular cancer cell lines: 833KE, Tera, and NCCIT. 833KE, Tera, and NCCIT cells showed a significant increase in apoptosis/cell death with the combination of AZD8055 and cisplatin in comparison to cisplatin alone (**Fig. 3A–C**). Western blot analysis of 833KE, Tera, and NCCIT cells confirmed the downregulation of the mTOR downstream proteins when treated with AZD8055 alone or in combination with cisplatin (**Fig. 3A–C**; Supplementary Fig. S4). Caspase-3 and PARP cleavage were induced by cisplatin treatment, and further increased by the combination of cisplatin with AZD8055 in all three cell lines (**Fig. 3D**).

Combined cisplatin and AZD8055 treatment induces caspase-dependent apoptosis in testicular cancer cells

We next investigated whether apoptosis induced by cisplatin and AZD8055 combination treatment was caspase dependent. Clearly, the percentages of cleaved caspase-3–positive Scha and TeraCP cells were elevated when cisplatin treatment was combined with AZD8055 (**Fig. 4A** and **B**). Addition of the pan-caspase inhibitor Z-VAD-FMK completely inhibited apoptosis and cell death induced by single and combined drug treatment, indicating that the observed drug-induced cell death was caspase dependent. Similar results were observed when flow cytometric analysis of DilC1(5)/PI uptake was used as read-out for apoptosis/cell death (**Fig. 4C** and **D**).

Combined cisplatin and AZD8055 treatment strongly reduces clonogenic survival in cisplatin-resistant testicular cancer cell lines

To determine whether mTORC1/2 inhibition in combination with cisplatin would hamper long-term clonogenic survival, Scha and TeraCP cells were pretreated with suboptimal concentrations of cisplatin for 24 hours and then incubated in presence of AZD8055. Cisplatin treatment reduced clonogenic survival of Scha and TeraCP in a concentration-dependent manner (**Fig. 5A** and **B**). Clonogenic survival of Scha or TeraCP cells was only reduced at the highest AZD8055 concentration used (**Fig. 5A** and **B**). Importantly, combined treatment with the highest doses of cisplatin and AZD8055 completely abolished clonogenic survival in both cell lines, whereas for Scha synergistic effects were only observed at the highest cisplatin concentration, we observed clear synergistic effects for all combinations in TeraCP (**Fig. 5C**).

Autophagy inhibition enhances apoptotic response to combined cisplatin and AZD8055 treatment

As mTOR is involved in the regulation of autophagy, we investigated whether autophagy was activated in our cell lines after AZD8055, cisplatin, or the combination treatment. Upon autophagy induction, LC3-I is converted to LC3-II via phosphatidylethanolamine

Published OnlineFirst November 19, 2019; DOI: 10.1158/1535-7163.MCT-19-0449

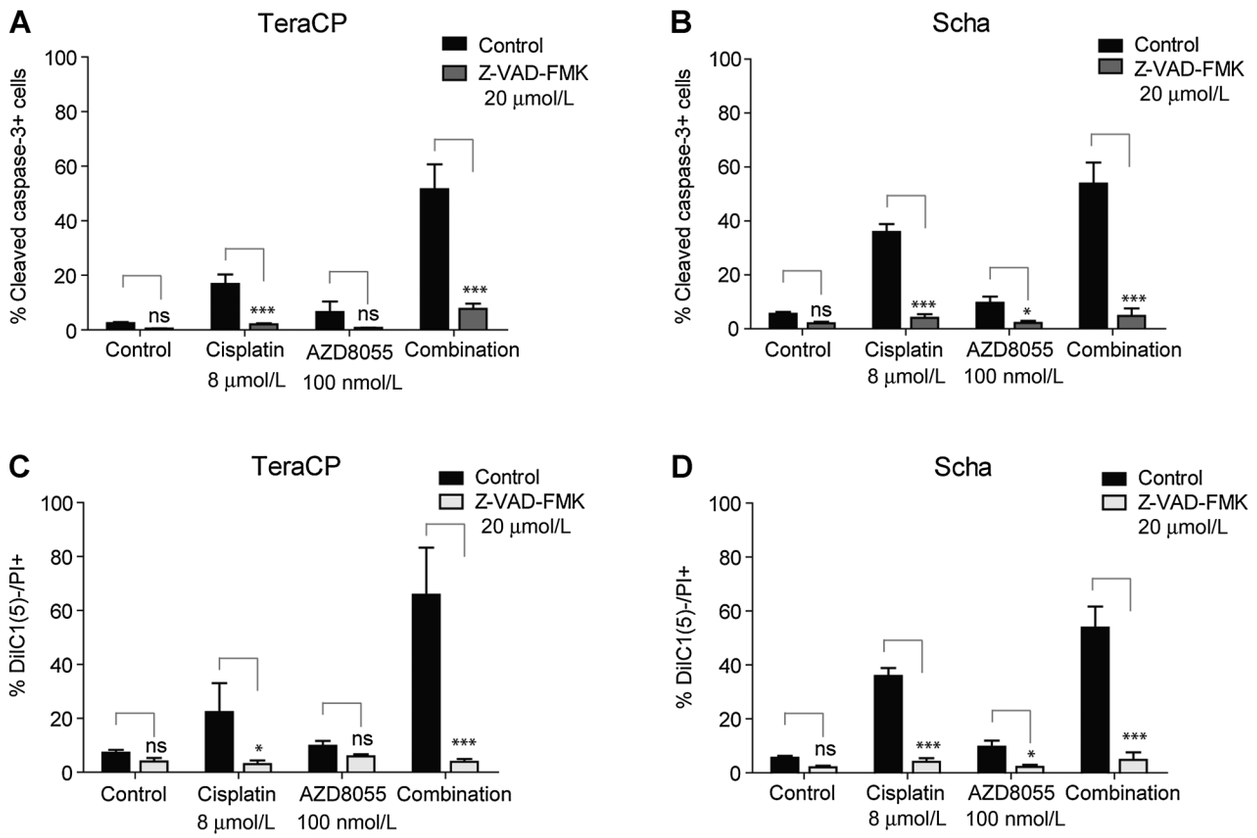

Figure 4.

Caspase inhibition in testicular cancer cells treated with cisplatin in combination with AZD8055. **A** and **B,** Mean percentage of apoptotic cells using TeraCP and Scha. **C** and **D,** Mean percentage of apoptotic and death cells using TeraCP and Scha. Data show average and ± SD of three different replicates. ANOVA was used to test significance, and pairwise comparisons were done using Sidak *post hoc* test. *, $P < 0.05$; **, $P < 0.01$; ***, $P < 0.001$; ns, not significant.

conjugation, and serves as a marker for autophagosome formation (17). We demonstrated that autophagy is activated in our cell line panel (except for 833KE) after AZD8055 or the combination treatment, indicated by increased levels of LC3-II (Supplementary Figs. S5B and S5C). We next investigated whether autophagy facilitates or inhibits apoptosis and cell death by using three well known autophagy inhibitors, the ULK1 inhibitor SBI-0206965, bafilomycin, and chloroquine. An increase in the percentage of apoptosis was observed for Scha and TeraCP cells when autophagy was inhibited using indicated drugs (Supplementary Fig. S5A). For TeraCP, inhibition of autophagy in control cells already caused an increase in apoptosis. These data suggest that autophagy affects the apoptotic response, acting as a protective antiapoptosis mechanism.

AZD8055 potentiates efficacy of cisplatin in testicular cancer PDX models

One cisplatin-sensitive (TC1) and one cisplatin-resistant (TC4) PDX model originating from nonseminoma testicular cancer tumors with wild-type *TP53* were treated with cisplatin, either alone or in combination with AZD8055 for 21 days. Suboptimal cisplatin doses were used in combination with AZD8055 (10 mg/kg/day). Change in tumor volume (**Fig. 6A** and **D**), and in final tumor volume (**Fig. 6B** and **E**) and tumor weight (**Fig. 6C** and **F**) at the end of the experiment were largest in the combination group of each PDX model as indicated by the statistically smaller tumor volume or weight with the combination therapy compared with treatment with cisplatin or the mTORC1/2 inhibitor. Mouse body weight was measured during the course of treatment as an indicator of toxicity. Only for PDX model TC4, receiving the highest dose of cisplatin, a decrease in body weight was observed in both the cisplatin and the combination treatment group (Supplementary Fig. S6A). None of the observed changes in body weight were significant, or exceeded the humane endpoint (>15% weight loss).

Tumor immunostaining for p-S6 revealed inhibition of the mTORC pathway in the TC4 model treated with AZD8055 alone, and in both models with the combination treatment (**Fig. 6I**). Immunostaining for p-4E-BP1 showed a similar pattern as p-S6 in TC1 and TC4 (Supplementary Figs. S6B and S6C). The percentage of Ki-67-positive nuclei decreased in the combination treatment group compared with the vehicle treatment group in the chemosensitive TC1 model, indicating a reduction in proliferation (**Fig. 6G**). Importantly, IHC analysis of cleaved caspase-3 demonstrated that addition of AZD8055 increased the amount of apoptotic cells only in the combination arm when compared with vehicle treatment in both PDX models (**Fig. 6H**).

Discussion

In this study, we show that testicular cancer models have a highly active PI3K/AKT/mTORC1/2 pathway and are very sensitive to

Published OnlineFirst November 19, 2019; DOI: 10.1158/1535-7163.MCT-19-0449

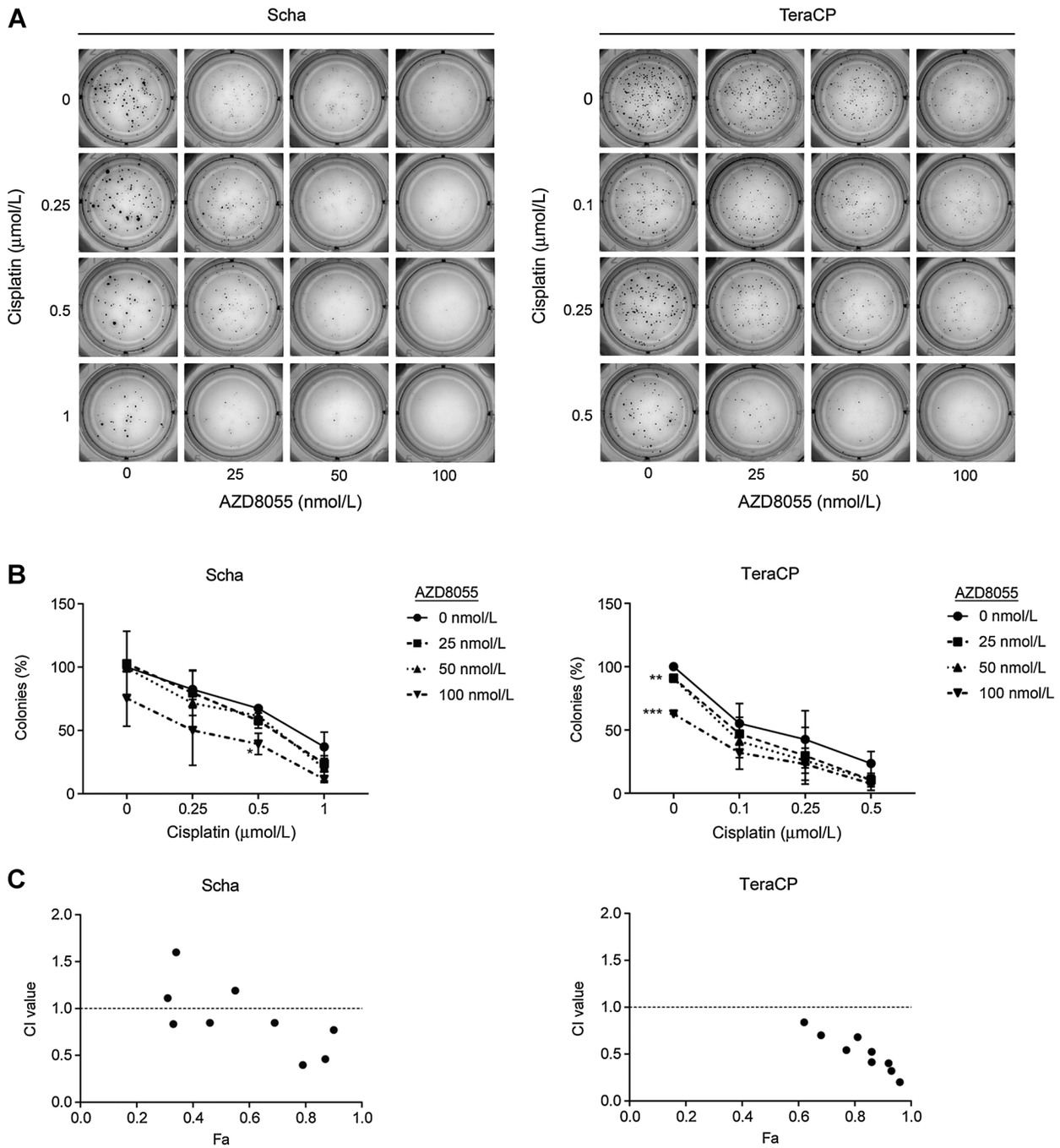

Figure 5.

Clonogenic survival in resistant testicular cancer cell lines. **A,** Representative images of a clonogenic survival assay using Scha and TeraCP cells in agarose after 10 to 12 days of incubation. Cells were pretreated for 24 hours with cisplatin and then seeded in the presence of AZD8055. Colonies were stained with MTT for 4 hours before imaging. **B,** Percentage of colonies in TeraCP and Scha treated as described in **A**. Two independent clonogenic survival experiments were performed and plated in triplicates. Error bars denote SEM. ANOVA was used to test significance, and pairwise comparisons were done using Dunnett *post hoc* test. **C,** Isobolograms generated by CompuSyn software showing synergy CI < 1, additive effects CI = 1, or antagonism CI > 1, for Scha and TeraCP. CI, combination index; Fa, fraction affected. *, $P < 0.05$; **, $P < 0.01$; ***, $P < 0.001$.

mTORC1/2 inhibition. Using intrinsic and acquired cisplatin-resistant models *in vitro*, we demonstrate that mTORC1/2 inhibition sensitizes cells to cisplatin-induced apoptosis and enhances cisplatin-induced growth inhibition. The *in vivo* experiments using clinically-relevant testicular cancer PDX models underscored the feasibility of this treatment strategy.

Here, we found that p-S6, p-AKT^{308}, and p-AKT^{473}, all belonging to the PI3K/AKT/mTORC pathway, were among the top phosphorylated

Published OnlineFirst November 19, 2019; DOI: 10.1158/1535-7163.MCT-19-0449

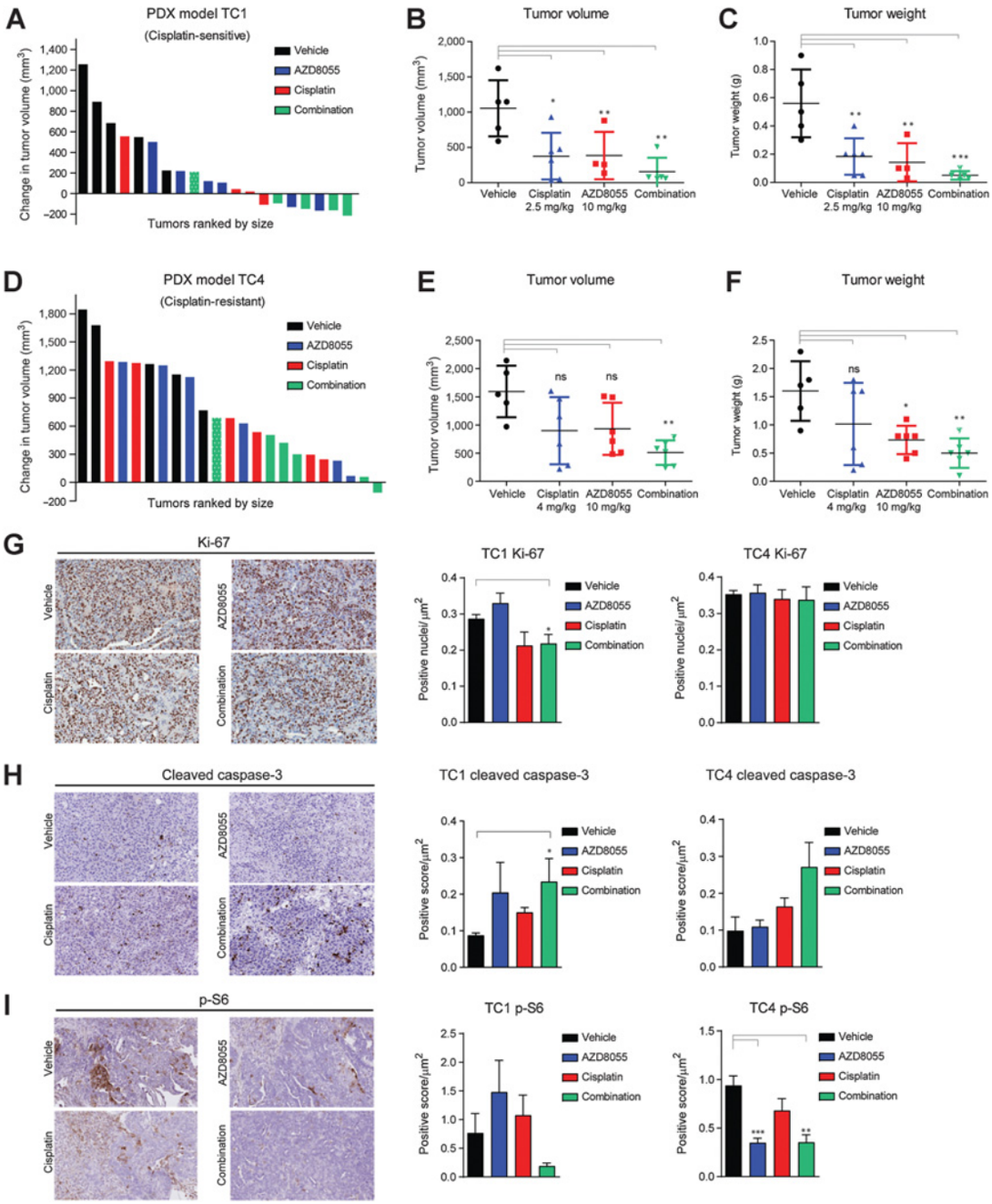

Figure 6.

mTORC1/2 inhibition in combination with cisplatin in testicular cancer PDX models. **A–F,** Tumor growth, final tumor volume, and tumor weight of each mouse from the chemosensitive (TC1) and chemoresistant (TC4) PDX models treated with vehicle, AZD8055, cisplatin, or the combination. Tumor growth was depicted as change in tumor volume (mm^3): tumor volume at the end of treatment—initial tumor volume. Dotted bars denote tumors that accumulated fluid, which might have influenced volume measurements. ANOVA was used to test significance, and pairwise comparisons were done using Dunnett *post hoc* test. Data show average ± SD. **G–I,** Representative images at 20× magnification and quantification of Ki-67 (TC4), cleaved caspase-3 (TC1), and p-S6 (TC4) IHC were made from tumors shown in **A–F**. Data show average ± SEM. *t* test was used to test significance between vehicle and combination groups. *, $P < 0.05$; **, $P < 0.01$; ***, $P < 0.001$; ns, not significant.

kinases in testicular cancer cell lines. Recently, it was shown that hyperactivation of the PI3K/AKT/mTORC pathway was linked to cisplatin resistance in testicular cancer models where resistant sublines showed higher levels of p-AKT^{473} compared with their sensitive parental cells (14, 18). The AKT-dependent cisplatin resistance in those testicular cancer models was found to be driven by PDGFRβ and IGF1R (14, 19). Our data show that the acquired-resistant subline TeraCP and its parental sensitive cell line Tera had similar p-AKT^{473}

Published OnlineFirst November 19, 2019; DOI: 10.1158/1535-7163.MCT-19-0449

and p-AKT^{308} levels. In addition, we did not observe any differences in PDGFRβ or IGF1R phosphorylation using kinase arrays (**Fig. 1C**) and even observed the highest PDGFRβ protein levels in Tera cells (Supplementary Fig. S7). The RTKs FGFR1, HER2, and HER3 were highly phosphorylated in our models. FGFR involvement in mTORC1 activation was previously shown in a large panel of seminoma and nonseminoma tumors (20). Together this indicates that independent of which upstream factor is involved in cisplatin sensitivity, the PI3K/AKT/mTORC pathway is activated in testicular cancer. Activation of the PI3K/AKT/mTORC pathway has been observed in patients with testicular cancer samples (8) and most of the genomic alterations seen in resistant disease like *K-RAS* and *N-RAS* activating mutations and *PTEN* loss, among others, can lead to its activation. Moreover, testicular cancer ranked among the tumor types with high activity of this pathway (8), indicating its importance as therapeutic target in testicular cancer. Remarkably, clinical data showed that chemoresistant compared with chemosensitive testicular cancer tumors do not exhibit more activating mutations in genes from the PI3K/AKT/mTORC pathway but rather in the p53–MDM2 axis, such as *TP53* mutations and *MDM2* amplifications (10, 11). Encouragingly, our results indicate that a *TP53* mutant testicular cancer model was also susceptible to mTORC1/2 inhibition added to cisplatin treatment.

Our results revealed that none of the PI3K/AKT/mTORC pathway inhibitors, targeting different kinases, induced apoptosis at concentrations that were shown to effectively block pathway activity. The mTORC1/2 inhibitors AZD8055 and MLN0128 most effectively enhanced cisplatin-induced apoptosis in all models. In contrast, knockdown of mTOR did not effectively block pathway activity, explaining why no sensitization to cisplatin-induced apoptosis was observed. These suggest that inhibition of the enzymatic activity of mTOR, rather than lowering mTOR protein levels, is essential for effective sensitization to cisplatin treatment. Two distinct complexes of mTOR with different cell function are known, for example mTORC1 and mTORC2. Although mTORC1 regulates cell metabolism, mTORC2 is involved in cell survival via phosphorylation of AKT at Ser473 (21). We found increased phosphorylation levels of AKT^{308} and AKT^{473} in cells treated with the mTORC1 inhibitor everolimus, suggesting the involvement of feedback loops (22). IRS-1–mediated AKT^{308} and AKT^{473} phosphorylation can be caused by the loss of the negative feedback loop via S6K1 when mTORC1 is inhibited by everolimus (23). In addition, a positive feedback loop between AKT and mTORC2 may result in a further enhancement of AKT activation (24), thus reducing the efficacy of everolimus. Dual inhibition of mTORC1/2 prevented the increase in p-AKT^{473} and to a lesser extent of p-AKT^{308}. Inhibition of these feedback loops may explain the higher sensitivity of testicular cancer cells to AZD8055 and MLN0128 compared with everolimus. In addition, these drugs induce autophagy via mTORC1 inhibition. Autophagy can be either a protective mechanism or a process that contributes to cell death (25). In our testicular cancer cell lines, blocking autophagy increased apoptosis levels, pointing towards a protective effect of autophagy in this context. Although the crosstalk between autophagy and apoptosis is complex, a role for the proapoptotic protein NOXA has been reported, showing that inhibition of autophagy increased NOXA protein levels and enhanced NOXA-mediated apoptosis (26). Interestingly, NOXA has been identified as an important mediator of cisplatin-induced apoptosis in testicular cancer cell lines (27). Nevertheless, despite the induction of autophagy, AZD8055 and MLN0128 still sensitized testicular cancer cells to cisplatin-induced apoptosis. The mechanism of sensitization needs to be further investigated, but suggests interactions with cisplatin activity either at the extrinsic or intrinsic apoptotic pathway, which are both known to be activated in testicular cancer models in response to cisplatin (27–29).

PDX models are being regarded as more accurate predictors of tumor response to drugs than cell line models (30, 31). This can be explained by their ability to recapitulate genomic alteration landscapes and resistance mechanisms seen in the clinic (32). Our testicular cancer PDX models established from chemosensitive primary testicular cancer and chemoresistant testicular cancer patient tumor tissue showed differences in cisplatin sensitivity, reflecting the clinical situation as well. Interestingly, in both PDX models cisplatin in combination with AZD8055 strongly reduced tumor growth and induced high levels of apoptosis, similar to our *in vitro* observations.

Recent reports showed that treatment with everolimus in refractory testicular cancer had limited efficacy (33), which is in line with mTORC1 inhibitors in other patients with advanced malignancies (34, 35). Several inhibitors of mTORC1/2, such as AZD8055, OSI-027, and MLN0128 (TAK-228) have been used in patients with cancer other than testicular cancer, but only the latter is still in clinical trials (NCT03430882, NCT02987959, NCT03097328). Assuring, we observed similar data with MLN0128 as compared with AZD8055. Cisplatin is the cornerstone of testicular cancer treatment. Until now, high-dose cisplatin-based chemotherapy and other regimens have been explored in patients with testicular cancer with several relapses or refractory disease (36–38) without clear evidence of improved survival compared with standard dose chemotherapy. Therefore, other combinations with cisplatin should be explored. Cytostatic drugs have been combined with kinase inhibitors and showed higher efficacy and tolerability in other cancer types in phase II trials (39, 40). In addition, feasibility of mTORC1/2 inhibition in combination with paclitaxel was assessed in a phase I clinical trial using MLN0128 (TAK-228/sapanisertib) in advanced solid malignancies with good tolerability and preliminary antitumor activity (41). There is no data available regarding the safety of combining cisplatin plus mTORC1/2 inhibitors in patients. However, a clinical trial with patients with triple negative breast cancer treated with the mTORC1 inhibitor everolimus in combination with cisplatin and paclitaxel showed increased toxicity when everolimus was added to the treatment. Therefore, safety issues involving cisplatin plus mTORC1/2 inhibitors still need to be addressed (42).

Taken together, our *in vitro* and *in vivo* results and the available clinical data support mTORC1/2 inhibitors in combination with cisplatin as a feasible approach in patients with testicular cancer with chemotherapy-resistant or refractory disease.

Disclosure of Potential Conflicts of Interest

M.A.T.M. van Vugt is a scientific advisory board member of RepareTx. No potential conflicts of interest were disclosed by the other authors.

Authors' Contributions

Conception and design: X. Rosas-Plaza, G. de Vries, M.A.T.M. van Vugt, S. de Jong
Development of methodology: X. Rosas-Plaza, G. de Vries, S. de Jong
Acquisition of data (provided animals, acquired and managed patients, provided facilities, etc.): X. Rosas-Plaza, G. de Vries, G.J. Meersma, A.J.H. Suurmeijer, J.A. Gietema
Analysis and interpretation of data (e.g., statistical analysis, biostatistics, computational analysis): X. Rosas-Plaza, G. de Vries, A.J.H. Suurmeijer, M.A.T.M. van Vugt, S. de Jong
Writing, review, and/or revision of the manuscript: X. Rosas-Plaza, G. de Vries, J.A. Gietema, M.A.T.M. van Vugt, S. de Jong
Administrative, technical, or material support (i.e., reporting or organizing data, constructing databases): X. Rosas-Plaza, G. de Vries, A.J.H. Suurmeijer
Study supervision: S. de Jong

Acknowledgments

The authors thank Joost J. Caumanns and Shang Li for help with the PDX models. S. de Jong is a member of the EurOPDX Consortium. This work was supported by a grant from the Dutch Cancer Society (RUG 2014-6691) to S. de Jong, M.A.T.M. van Vugt, and J.A. Gietema, and by a grant from Conacyt (381543) to X. Rosas-Plaza.

The costs of publication of this article were defrayed in part by the payment of page charges. This article must therefore be hereby marked *advertisement* in accordance with 18 U.S.C. Section 1734 solely to indicate this fact.

Received April 25, 2019; revised September 13, 2019; accepted November 7, 2019; published first November 19, 2019.

References

1. Giannandrea F, Fargnoli S. Environmental factors affecting growth and occurrence of testicular cancer in childhood: an overview of the current epidemiological evidence. Children 2017;4:1.
2. Hanna NH, Einhorn LH. Testicular cancer - discoveries and updates. N Engl J Med 2014;371:2005–16.
3. Einhorn LH. Curing metastatic testicular cancer. Proc Natl Acad Sci U S A 2002; 99:4592–5.
4. Welsh C, Day R, McGurk C, Masters JRW, Wood RD, Köberle B. Reduced levels of XPA, ERCC1 and XPF DNA repair proteins in testis tumor cell lines. Int J Cancer 2004;110:352–61.
5. Vousden KH, Lu X. Live or let die: the cell's response to p53. Nat Rev Cancer 2002;2:594–604.
6. Koster R, van Vugt MATM, Timmer-Bosscha H, Gietema JA, de Jong S. Unravelling mechanisms of cisplatin sensitivity and resistance in testicular cancer. Expert Rev Mol Med 2013;15:e12.
7. Montero J, Sarosiek KA, DeAngelo JD, Maertens O, Ryan J, Ercan D, et al. Drug-induced death signaling strategy rapidly predicts cancer response to chemotherapy. Cell 2015;160:977–89.
8. Zhang Y, Kwok-Shing Ng P, Kucherlapati M, Chen F, Liu Y, Tsang YH, et al. A pan-cancer proteogenomic atlas of PI3K/AKT/mTOR pathway alterations. Cancer Cell 2017;31:820–32.
9. Thorpe LM, Yuzugullu H, Zhao JJ. PI3K in cancer: divergent roles of isoforms, modes of activation and therapeutic targeting. Nat Rev Cancer 2015;15:7–24.
10. Bagrodia A, Lee BH, Lee W, Cha EK, Sfakianos JP, Iyer G, et al. Genetic determinants of cisplatin resistance in patients with advanced germ cell tumors. J Clin Oncol 2016;34:4000–7.
11. Litchfield K, Levy M, Huddart RA, Shipley J, Turnbull C. The genomic landscape of testicular germ cell tumours: from susceptibility to treatment. Nat Rev Urol 2016;13:409–19.
12. Shen H, Shih J, Hollern DP, Wang L, Bowlby R, Tickoo SK, et al. Integrated molecular characterization of testicular germ cell tumors. Cell Rep 2018;23: 3392–406.
13. Koster R, di Pietro A, Timmer-Bosscha H, Gibcus JH, van den Berg A, Suurmeijer AJ, et al. Cytoplasmic p21 expression levels determine cisplatin resistance in human testicular cancer. J Clin Invest 2010;120: 3594–605.
14. Selfe J, Goddard NC, McIntyre A, Taylor KR, Renshaw J, Popov SD, et al. IGF1R signalling in testicular germ cell tumour cells impacts on cell survival and acquired cisplatin resistance. J Pathol 2018;244:242–53.
15. Alkema NG, Tomar T, Duiker EW, Jan Meersma G, Klip H, van der Zee AGJ, et al. Biobanking of patient and patient-derived xenograft ovarian tumour tissue: efficient preservation with low and high fetal calf serum based methods. Sci Rep 2015;5:14495.
16. Voutsadakis IA. The chemosensitivity of testicular germ cell tumors. Cell Oncol 2014;37:79–94.
17. Klionsky DJ, Abdelmohsen K, Abe A, Abedin MJ, Abeliovich H, Arozena AA, et al. Guidelines for the use and interpretation of assays for monitoring autophagy (3rd edition). Autophagy 2016;12:1.
18. Juliachs M, Vidal A, Del Muro XG, Piulats JM, Condom E, Casanovas O, et al. Effectivity of pazopanib treatment in orthotopic models of human testicular germ cell tumors. BMC Cancer 2013;13:382.
19. Juliachs M, Muñoz C, Moutinho CA, Vidal A, Condom E, Esteller M, et al. The PDGFRβ-AKT pathway contributes to CDDP-acquired resistance in testicular germ cell tumors. Clin Cancer Res 2014;20:658–67.
20. Chen KS, Fustino NJ, Shukla AA, Stroup EK, Budhipramono A, Ateek C, et al. EGF receptor and mTORC1 are novel therapeutic targets in nonseminomatous germ cell tumors. Mol Cancer Ther 2018;17:1079–89.
21. Chiarini F, Evangelisti C, McCubrey JA, Martelli AM. Current treatment strategies for inhibiting mTOR in cancer. Trends Pharmacol Sci 2015;36: 124–35.
22. Saxton RA, Sabatini DM. mTOR signaling in growth, metabolism, and disease. Cell 2017;168:960–76.
23. Showkat M, Beigh MA, Andrabi KI. mTOR signaling in protein translation regulation: implications in cancer genesis and therapeutic interventions. Mol Biol Int 2014;2014:686984.
24. Yang G, Murashige DS, Humphrey SJ, James DE. A positive feedback loop between Akt and mTORC2 via SIN1 phosphorylation. Cell Rep 2015;12: 937–43.
25. Debnath J, Baehrecke EH, Kroemer G. Does autophagy contribute to cell death? Autophagy 2005;1:66–74.
26. Wang J, Cui D, Gu S, Chen X, Bi Y, Xiong X, et al. Autophagy regulates apoptosis by targeting NOXA for degradation. Biochem Biophys Acta 2018;8: 1105–13.
27. Gutekunst M, Mueller T, Weilbacher A, Dengler MA, Bedke J, Kruck A, et al. Cisplatin hypersensitivity of testicular germ cell tumors is determined by high constitutive noxa levels mediated by Oct-4. Cancer Res 2013;5:1460–9.
28. Spierings DCJ, de Vries EGE, Stel AJ, te Rietstap N, Vellenga E, de Jong S. Low p21Waf1/Cip1 protein level sensitizes testicular germ cell tumor cells to Fas-mediated apoptosis. Oncogene 2004;23:4862–72.
29. Mueller T, Voigt W, Simon H, Fruehauf A, Bulankin A, Grothey A, et al. Failure of activation of caspase-9 induces a higher threshold for apoptosis and cisplatin resistance in testicular cancer. Cancer Res 2003;63:513–21.
30. Gao H, Korn JM, Ferretti S, Monahan JE, Wang Y, Singh M, et al. High-throughput screening using patient-derived tumor xenografts to predict clinical trial drug response. Nat Med 2015;21:1318–25.
31. Yu J, Qin B, Moyer AM, Sinnwell JP, Thompson KJ, Copland JA, et al. Establishing and characterizing patient-derived xenografts using pre-chemotherapy percutaneous biopsy and post-chemotherapy surgical samples from a prospective neoadjuvant breast cancer study. Breast Cancer Res 2017; 19:130.
32. Krepler C, Sproesser K, Brafford P, Schuchter L, Nathanson KL, Herlyn M. A comprehensive patient-derived xenograft collection representing the heterogeneity of melanoma. Cell Rep 2017;21:1953–67.
33. Mego M, Svetlovska D, Miskovska V, Obertova J, Palacka P, Rajec J, et al. Phase II study of everolimus in refractory testicular germ cell tumors. Urol Oncol 2016; 34:122.e17–e22.
34. Mita MM, Poplin E, Britten CD, Tap WD, Rubin EH, Scott BB, et al. Phase I/IIa trial of the mammalian target of rapamycin inhibitor ridaforolimus (AP23573; MK-8669) administered orally in patients with refractory or advanced malignancies and sarcoma. Ann Oncol 2013;24:1104–11.
35. Amato RJ, Wilding G, Bubley G, Loewy J, Haluska F, Gross ME. Safety and preliminary efficacy analysis of the mTOR inhibitor ridaforolimus in patients with taxane-treated, castration-resistant prostate cancer. Clin Genitourin Cancer 2012;10:232–8.
36. Fizazi K, Gravis G, Flechon A, Geoffrois L, Chevreau C, Laguerre B, et al. Combining gemcitabine, cisplatin, and ifosfamide (GIP) is active in patients with relapsed metastatic germ-cell tumors (GCT): a prospective multicenter GETUG phase II trial. Ann Oncol 2014;25:987–91.
37. Pico JL, Rosti G, Kramar A, Wandt H, Koza V, Salvioni R, et al. A randomised trial of high-dose chemotherapy in the salvage treatment of patients failing first-line platinum chemotherapy for advanced germ cell tumours. Ann Oncol 2005; 16:1152–9.
38. Necchi A, Nicolai N, Mariani L, Lo Vullo S, Giannatempo P, Raggi D, et al. Combination of paclitaxel, cisplatin, and gemcitabine (TPG) for multiple relapses or platinum-resistant germ cell tumors: long-term outcomes. Clin Genitourin Cancer 2014;12:63–9.
39. Yap TA, Omlin A, de Bono JS. Development of therapeutic combinations targeting major cancer signaling pathways. J Clin Oncol 2013;31:1592–605.
40. Marty M, Cognetti F, Maraninchi D, Snyder R, Mauriac L, Tubiana-Hulin M, et al. Randomized phase II trial of the efficacy and safety of trastuzumab combined with docetaxel in patients with human epidermal growth factor

receptor 2–positive metastatic breast cancer administered as first-line treatment: the M77001 study group. J Clin Oncol 2005;23:4265–74.
41. Burris HA, Kurkjian CD, Hart L, Pant S, Murphy PB, Jones SF, et al. TAK-228 (formerly MLN0128), an investigational dual TORC1/2 inhibitor plus paclitaxel, with/without trastuzumab, in patients with advanced solid malignancies. Cancer Chemother Pharmacol 2017;80:261–73.
42. Jovanović B, Mayer IA, Mayer EL, Abramson VG, Bardia A, Sanders ME, et al. A randomized phase II neoadjuvant study of cisplatin, paclitaxel with or without everolimus in patients with stage II/III triple-negative breast cancer (TNBC): responses and long-term outcome correlated with increased frequency of DNA damage response gene. Clin Cancer Res 2017;23:4035–45.

Published OnlineFirst November 19, 2019; DOI: 10.1158/1535-7163.MCT-19-0449

Molecular Cancer Therapeutics

Dual mTORC1/2 Inhibition Sensitizes Testicular Cancer Models to Cisplatin Treatment

Ximena Rosas-Plaza, Gerda de Vries, Gert Jan Meersma, et al.

Mol Cancer Ther 2020;19:590-601. Published OnlineFirst November 19, 2019.